RadioGraphics

CT and MR Imaging of the Adrenal Glands in ACTH-independent Cushing Syndrome[1]

Andrea G. Rockall, FRCR • Syed A. Babar, FRCR • S. A. Aslam Sohaib, FRCR[2] • Andrea M. Isidori, MD • Salvador Diaz-Cano, MD, PhD • John P. Monson, MD • Ashley B. Grossman, MD • Rodney H. Reznek, FRCR

CME FEATURE

See accompanying test at http://www.rsna.org/education/rg_cme.html

LEARNING OBJECTIVES FOR TEST 4

After reading this article and taking the test, the reader will be able to:

- List the primary adrenal diseases that may cause ACTH-independent Cushing syndrome.
- Describe the characteristic imaging features of these diseases.
- Discuss the correlation between the imaging and histologic features of these diseases.

Adrenocorticotropic hormone (ACTH)–independent hypercortisolism accounts for 15%–20% of cases of Cushing syndrome and always arises from primary adrenal disease. Computed tomographic (CT) and magnetic resonance (MR) imaging findings in 37 patients with primary adrenal Cushing syndrome were analyzed and correlated with pathologic findings. Hyperfunctioning adenomas ($n = 24$), together with functioning carcinomas ($n = 10$), accounted for 92% of cases. Adenomas had a significantly smaller mean size (3.5 vs 14.5 cm) and lower mean unenhanced CT attenuation value (11 vs 28 HU) than did carcinomas. The presence of necrosis, hemorrhage, and calcification favored a diagnosis of carcinoma. Six of 10 carcinoma patients had metastases at presentation. Two adenomas were seen within a myelolipoma, which was recognized at both CT and MR imaging due to its fat content, and two adenomas were of uncertain malignant potential. Bilateral disease—primary pigmented nodular adrenal dysplasia (PPNAD) ($n = 2$) and ACTH-independent macronodular adrenal hyperplasia (AIMAH) ($n = 1$)—had characteristic imaging features. In PPNAD, multiple tiny (2–5-mm) nodules were visible bilaterally, with no overall glandular enlargement and normal intervening adrenal tissue. In AIMAH, both glands were grossly enlarged and contained nodules up to 3 cm in diameter. Familiarity with the range of imaging appearances of the adrenal glands in primary adrenal Cushing syndrome may help establish the underlying diagnosis.

Abbreviations: ACTH = adrenocorticotropic hormone, AIMAH = ACTH-independent macronodular adrenal hyperplasia, FMPSPGR = fast multiplanar spoiled gradient-echo, GIP = gastric inhibitory polypeptide, H-E = hematoxylin-eosin, IVC = inferior vena cava, PPNAD = primary pigmented nodular adrenal dysplasia

Index terms: Adrenal gland, CT, 86.1211 • Adrenal gland, diseases, 86.54 • Adrenal gland, MR, 86.12141 • Adrenal gland, neoplasms, 86.31, 86.32 • Cushing syndrome, 86.541

RadioGraphics 2004; 24:435–452 • **Published online** 10.1148/rg.242035092

[1]From the Departments of Academic Radiology (A.G.R., S.A.B., S.A.A.S., R.H.R.), Endocrinology (A.M.I., J.P.M., A.B.G.), and Histopathology (S.D.C.), St Bartholomew's Hospital, Dominion House, St Bartholomew's Close, London EC1A 7ED, England. Presented as an education exhibit at the 2002 RSNA scientific assembly. Received April 2, 2003; revision requested May 7 and received June 12; accepted June 13. All authors have no financial relationships to disclose. **Address correspondence to** A.G.R. (e-mail: *a.g.rockall@qmul.ac.uk*).

[2]Current address: Department of Radiology, Royal Marsden Hospital, London, England.

Introduction

Cushing syndrome is the clinical manifestation of hypercortisolism and is most frequently iatrogenic. Endogenous Cushing syndrome is a relatively rare disease and may be adrenocorticotropic hormone (ACTH)–dependent (80%–85% of cases) or ACTH-independent (15%–20%) (1). ACTH-dependent Cushing syndrome is due to an ACTH-secreting pituitary adenoma (Cushing disease) in approximately 75%–85% of cases. Rarely, an ectopic source of ACTH may cause ACTH-dependent Cushing syndrome (1,2). The appearance of the adrenal glands in ACTH-dependent Cushing syndrome has been described previously (2).

ACTH-independent Cushing syndrome is always caused by primary adrenal disease (1). The hyperfunctioning primary adrenal disease secretes cortisol and results in Cushing syndrome. ACTH-independent Cushing syndrome is due to an adenoma or carcinoma in the majority of cases but on rare occasions may be caused by other diseases, including primary pigmented nodular adrenal dysplasia (PPNAD) and ACTH-independent macronodular hyperplasia (AIMAH) (3,4). Cross-sectional imaging is used to identify adrenal disease in the investigation of Cushing syndrome. To our knowledge, however, there are no large series describing the imaging features of ACTH-independent Cushing syndrome.

In this article, we describe the range of imaging appearances of primary adrenal diseases that can cause ACTH-independent Cushing syndrome. We discuss and illustrate both unilateral disease (adenoma, adenoma within a myelolipoma, adenoma of uncertain malignant potential, carcinoma) and bilateral disease (PPNAD, AIMAH).

Patients and Procedures

Patients

Cases were drawn from those entered in the database of patients with Cushing syndrome in the Department of Endocrinology at our institution. Between January 1964 and October 2001, 413 patients with Cushing syndrome were evaluated in the Department of Endocrinology, and the case notes were entered in the database according to the cause of hypercortisolism. Patients without a definitive diagnosis for the cause of hypercortisolism (ie, Cushing syndrome of "unknown etiology") were not included. Of these 413 patients, 95 (23%) had ACTH-independent Cushing syndrome, and of these 95 patients, 60 (63%) had an adrenal adenoma, 30 (32%) had an adrenal carcinoma, five (5%) had AIMAH, and two (2%) had PPNAD. Results of cross-sectional imaging were available in 37 patients, who formed the study population. Several cases in the database had been referred from outside hospitals, and the scans were not available for review. The gender, mean age, and age range of these 37 patients are summarized in Table 1.

Diagnosis of ACTH-independent Cushing Syndrome

The diagnosis of Cushing syndrome was based on the clinical features of hypercortisolism, absence of serum cortisol diurnal rhythm, elevated midnight sleeping cortisol levels, and incomplete suppression of cortisol after an oral 2-mg 48-hour low-dose dexamethasone suppression test (standard protocol) to test for suppression of plasma cortisol or urinary steroids (5). A diagnosis of primary adrenal Cushing syndrome was made on the basis of clinical, biochemical, hormonal, and histopathologic criteria. The diagnostic biochemical feature was taken to be the presence of persistently undetectable (<10 pg/mL) levels of ACTH on several samples obtained throughout the day and, when available, after corticotropin-releasing hormone stimulation. Other features that suggested adrenal Cushing syndrome included *(a)* failure to suppress urinary or plasma cortisol levels during both low- and high-dose dexamethasone suppression tests and *(b)* failure of serum cortisol to respond to the corticotropin-releasing hormone stimulation test.

Table 1
Gender and Age in Study Patients

Diagnosis	No. of Patients	Gender		Age (y)	
		Male	Female	Mean	Range
Adenoma	20	7	13	45	5–66
Adenoma within a myelolipoma	2	0	2	55	44–65
Adenoma of uncertain malignant potential	2	1	1	72	71–73
Carcinoma	10	3	7	43	11–67
PPNAD	2	1	1	19	10–28
AIMAH	1	1	0	50	. . .*
All	37	12	25	45	5–73

*Not applicable.

Imaging Considerations

The computed tomographic (CT) and magnetic resonance (MR) imaging techniques varied considerably due to the long period over which the data were collected. CT scans and MR images were both available in 15 patients, CT scans alone in 19, and MR images alone in three. CT scans and MR images were reviewed either on hard copy or, if the equipment was available, loaded onto an independent viewing console (GE Medical Systems, Waukesha, Wis) from the digital archives. The images were reviewed by two experienced observers, who arrived at a consensus. Imaging characteristics were recorded, including lesion size and shape; presence or absence of calcification, hemorrhage, and necrosis; enhancement pattern; and signal intensity change at chemical shift imaging.

Histologic Analysis

Results of histopathologic analysis were available in 36 of the 37 patients. Surgery was not considered appropriate in one patient because she presented with a large necrotic adrenal mass with extensive metastases and had clinical findings that were consistent with an adrenal carcinoma. All surgical specimens were fixed in 10% buffered formaldehyde and routinely processed for histologic diagnosis. The lesions were sampled by taking at least one block per centimeter of maximum diameter. All microscopic slides were reviewed to assess the morphologic criteria of malignancy while keeping the presence of metastases as the main criterion for malignancy (6). The morphologic classification of adrenal cortical hyperplasia took into account the nodule size, pattern of distribution, color, and architectural pattern (7).

Results

Of the 37 patients, 20 had an adenoma, two had an adenoma within a myelolipoma, two had an adenoma of uncertain malignant potential, 10 had a carcinoma, two had PPNAD, and one had AIMAH. The mean age and age range for patients in each category are shown in Table 1. Mean age did not differ significantly between categories, although the mean age of the two patients with PPNAD was lower than that of patients in the other categories. However, the numbers were too small for formal statistical analysis.

Table 2
Imaging Characteristics of Unilateral Adrenal Masses Causing ACTH-independent Cushing Syndrome

Mass	Side*	Maximum Diameter (cm)†	Physical Characteristics	Unenhanced Texture	Unenhanced CT Attenuation (HU)†	Contrast Enhancement
Adenoma ($n = 20$)	11, 9	3.5, 2–7	Ovoid ($n = 12$), round ($n = 2$), lobulated ($n = 6$); contained blood ($n = 1$)	Homogeneous ($n = 10$), mildly heterogeneous ($n = 10$)	10.9, −16–41	Mild, slightly heterogeneous
Adenoma within a myelolipoma ($n = 2$)	1, 1	7.4, 7.2–7.6	Lobulated; contained blood ($n = 1$)	Moderately heterogeneous	−41.5, −92–9	Mild, slightly heterogeneous
Adenoma of uncertain malignant potential ($n = 2$)	1, 1	5, 3.5–6.5	Ovoid ($n = 1$), lobulated ($n = 1$); contained foci of fat attenuation ($n = 2$) and calcification ($n = 1$)	Mildly heterogeneous	38, NA‡	Moderate, slightly heterogeneous
Carcinoma ($n = 10$)	4, 6	14.5, 7.5–21	Ovoid ($n = 1$), lobulated ($n = 9$); contained necrosis ($n = 9$), blood ($n = 4$), and calcification ($n = 3$)	Markedly heterogeneous	28.1, 20–31	Variable, markedly heterogeneous

Note.—Difference in CT attenuation between adenoma and carcinoma, $P = .048$ (Kruskal-Wallis test); difference in nodule size between adenoma and carcinoma, $P < .0001$ (Kruskal-Wallis test).
*Values represent number of neoplasms on the right and left sides.
†Values represent mean and range.
‡NA = not available; measurement in Hounsfield units was possible in only one case.

Table 3
Imaging Characteristics of Diffuse Bilateral Disease Causing ACTH-independent Cushing Syndrome

Disease	Limb Width (mm)	Maximum Nodule Size (mm)	Contour	Unenhanced Texture	Enhancement	Findings of Blood, Fat, Calcification, or Necrosis
PPNAD ($n = 2$)	2–5	5	Nodular	Homogeneous	Moderate	None
AIMAH ($n = 1$)	30	30	Nodular	Homogeneous	Intense	None

Table 4
MR Imaging Characteristics of Adrenal Lesions Causing ACTH-independent Cushing Syndrome

Lesion	Signal Intensity at T1-weighted Imaging	Signal Intensity at T2-weighted Imaging	Signal Dropout* at Chemical Shift Imaging (%)†
Adenoma (n = 8)	Greater than or equal to muscle in all eight cases, less than or equal to liver in seven cases, greater than or equal to spleen in seven cases	Greater than or equal to muscle and liver in all seven cases, less than or equal to spleen in six cases	43.7, 0–73
Adenoma within a myelolipoma (n = 2)	Greater than or equal to muscle in both cases, less than liver in one case and more than liver in one case, greater than or equal to spleen in both cases	Less than muscle, liver, and spleen in one case; greater than muscle, liver, and spleen in one case	46.3, N/A‡
Adenoma of uncertain malignant potential (n = 2)	Equal to muscle in both cases, less than or equal to liver and spleen in both cases	Greater than muscle and liver in both cases, equal to spleen in both cases	6.5, 4–9
Carcinoma (n = 5)	Greater than or equal to muscle in all five cases, less than or equal to liver in all five cases, less than or equal to spleen in four cases	Greater than muscle and liver in all five cases, less than or equal to spleen in four cases	N/A
PPNAD (n = 1)	Greater than muscle, equal to liver, greater than spleen	Greater than muscle and liver, equal to spleen	40, . . .§
AIMAH (n = 1)	Equal to muscle, less than liver, equal to spleen	Greater than muscle, liver, and spleen	42, . . .

*Between in-phase and out-of-phase images.
†Values represent mean and range.
‡NA = not available.
§Not applicable.

The CT and MR imaging features of the various adrenal lesions are shown in Tables 2–4.

Unilateral Adrenal Disease

The observers were able to identify the nodule or mass in every case of unilateral adrenal disease (Tables 2, 4).

Adenoma.—An adenoma was confirmed in 20 of 37 cases. The adenomas had a female predilection, and the mean age of affected patients was 45 years (range, 5–66 years). The lesion was usually ovoid, with a mean diameter of 3.5 cm (range, 2–7 cm). The mean CT attenuation value was low (11 HU; range, −16–41 HU); one-half of the nodules were homogeneous, whereas one-half were slightly heterogeneous. A trace of blood was seen in only one case (at MR imaging). Calcification and necrosis were absent in all cases. Following intravenous administration of contrast

Figure 1. Adrenal adenoma in a 68-year-old man. **(a)** Unenhanced CT scan shows a smooth, ovoid, well-defined low-attenuation mass (arrow). The CT attenuation value was −5 HU, indicating the presence of intracellular lipid. Korobkin et al (8) demonstrated a cut-off point of 18 HU, below which an adrenal lesion may be designated as a benign adenoma with a specificity of 85% and a sensitivity of 100%. **(b)** Contrast material–enhanced CT scan shows moderate enhancement of the mass (arrow), which gives the lesion a slightly heterogeneous appearance. **(c)** Axial in-phase (repetition time msec/echo time msec = 150/4.2) (top) and out-of-phase (150/1.8) (bottom) fast multiplanar spoiled gradient-echo (FMPSPGR) T1-weighted MR images (flip angle = 90°) show the mass with classic signal dropout (arrow), a finding that suggests the presence of intracellular lipid, a characteristic feature of benign adenomas. **(d)** On an axial fast spin-echo T2-weighted MR image (6,000/105), the adenoma (arrow) is isointense relative to the liver. **(e)** High-power photomicrograph (original magnification, ×400; hematoxylin-eosin [H-E] stain) demonstrates a lipid-rich adrenal adenoma with abundant intracellular fat (arrow).

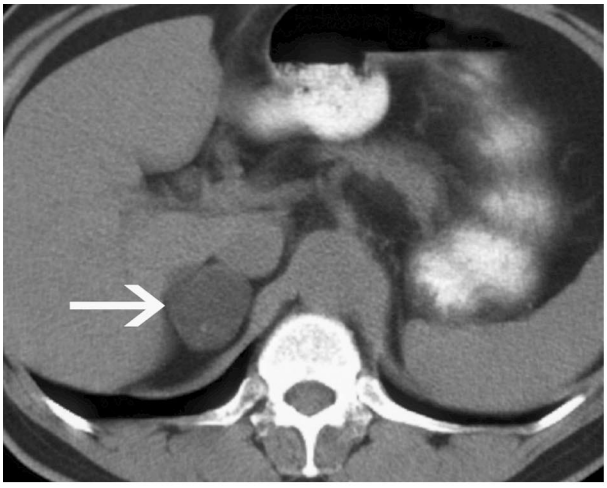

a.

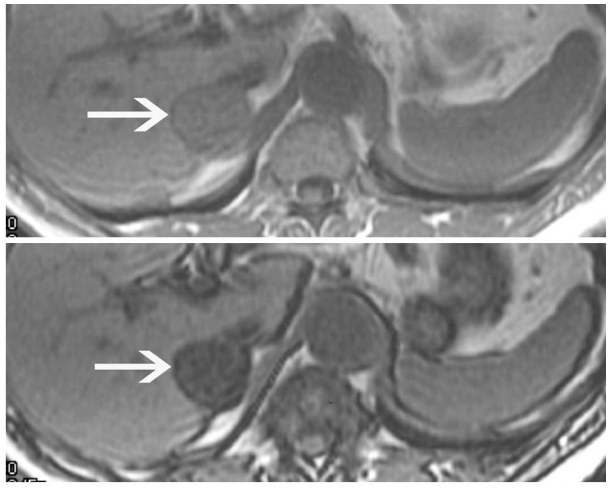

c.

b.

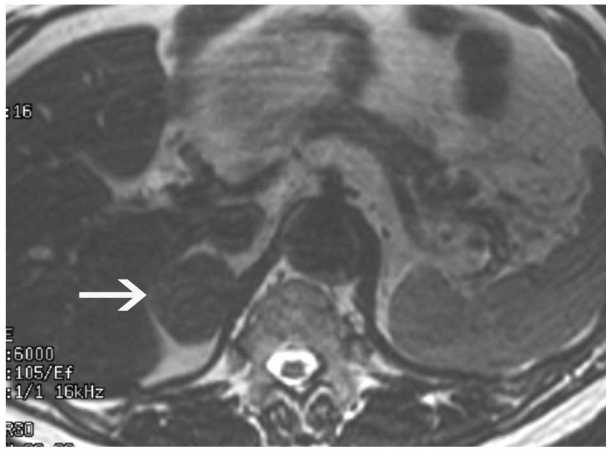

d.

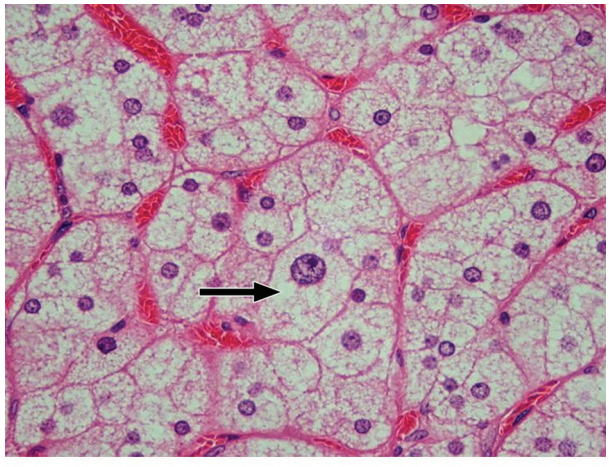

e.

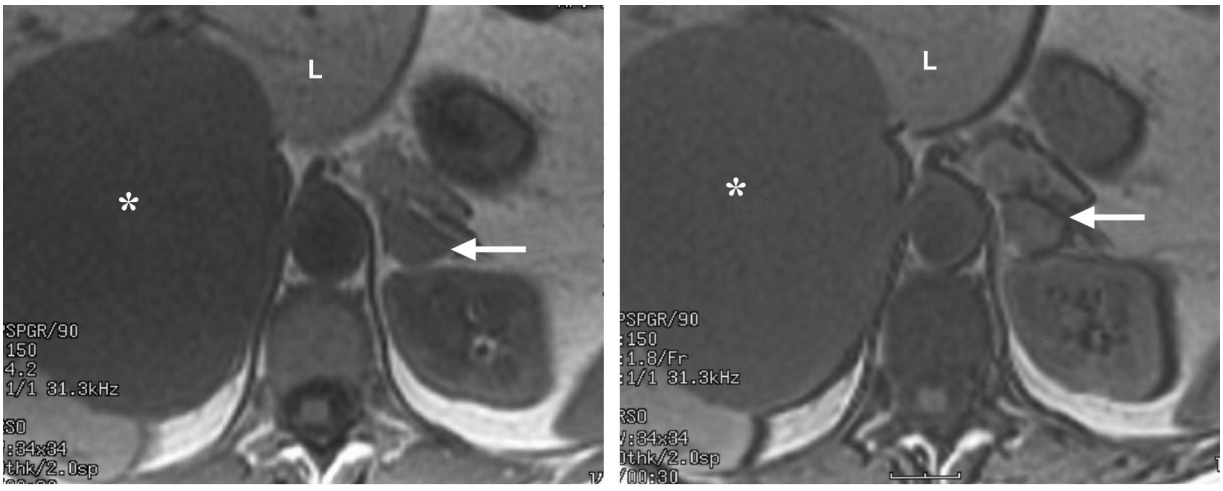

a. b.

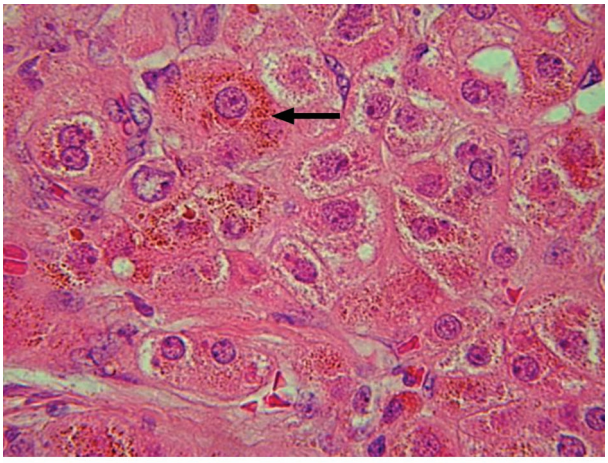

c.

Figure 2. Small adenoma in a 51-year-old woman. **(a)** Axial in-phase FMPSPGR T1-weighted MR image (150/4.2, flip angle = 90°) shows an ovoid mass that arises from the medial limb of the left adrenal gland (arrow). A large hemangioma (*) was seen incidentally in the liver *(L)*. **(b)** Axial out-of-phase FMPSPGR T1-weighted MR image (150/1.8, flip angle = 90°) shows no signal dropout in the mass (arrow). This finding is uncharacteristic of adenomas, which classically show signal dropout with the out-of-phase sequence. *L* = liver, * = hemangioma. **(c)** Photomicrograph (original magnification, ×400; H-E stain) shows a lipid-poor adrenal adenoma that contains predominantly eosinophilic compact cells with abundant lipofuscin pigment, which appears brown (arrow). These histologic findings may account for the lack of signal dropout in **b**.

material, either at CT or MR imaging, there was only mild to moderate and slightly heterogeneous enhancement in all cases (Fig 1). At chemical shift imaging, the mean signal dropout was 43.7% (range, 0%–73%) (Fig 1). In one adenoma, there was no signal dropout, and histologic analysis revealed a markedly pigmented and lipid-poor cortical adenoma (Fig 2). In one case, the patient presented with Conn syndrome and was also found to be hypercortisolemic; a cortical adrenal adenoma that was secreting both cortisol and aldosterone was identified (9). In this case, there was marked signal dropout at chemical shift imaging, a finding that is typical of a lipid-rich adenoma.

Adenoma within a Myelolipoma.—In two of 37 cases, imaging demonstrated an adrenal myelolipoma. In both cases, an adrenal cortical adenoma was found within the myelolipoma at histologic analysis. The diagnosis of myelolipoma

Figure 3. Adenoma within a myelolipoma in a 44-year-old woman with Cushing syndrome. **(a)** Longitudinal ultrasonographic image shows a hyperechoic suprarenal mass (arrow) with an appearance consistent with that of a predominantly fat-containing lesion. **(b)** Unenhanced CT scan helps confirm the fatty nature of the mass (arrow). However, a relatively large soft-tissue component (*) can also be seen within the lesion. **(c)** Coronal spin-echo T1-weighted MR images (740/25) show a predominantly fat-containing high-signal-intensity mass (short arrows) with areas of intermediate signal intensity (long arrow). **(d)** Axial short inversion time inversion-recovery MR image (1,800/25, inversion time msec = 100) shows a large mass with marked signal dropout (arrow), a finding that confirms the predominantly fatty nature of the lesion. At histologic analysis, the lesion proved to be a myelolipoma containing an adenoma.

was made at imaging based on the presence of clearly visible fat in the lesion (Fig 3). However, in both cases, there had been concern at the time of diagnosis over the relatively large amount of soft tissue within these lesions and the size of the lesions (7.2 and 7.6 cm, respectively), findings that raise the possibility of malignant potential (Fig 4). At histologic analysis, the nonfatty soft-tissue component was seen to represent a cortical adenoma in both cases, although in one case, histopathologic findings suggested that the lesion was of uncertain malignant potential due to its size.

Figure 4. Adenoma associated with a myelolipoma in a 64-year-old woman with Cushing syndrome. **(a)** Axial unenhanced CT scan shows a large left adrenal mass with multiple low-attenuation areas centrally (horizontal arrow) that represent pockets of fat. A speck of calcification (vertical arrow) is also noted adjacent to the fatty component. **(b)** Contrast-enhanced arterial-phase CT scan shows mild enhancement of the mass. **(c)** Axial spin-echo T1-weighted MR image (500/16) shows the mass with small central foci of high signal intensity (arrow) that correspond to the foci of fat seen at CT. **(d)** Axial fast spin-echo T2-weighted MR image (6,000/102) shows the mass with mixed signal intensity. Multiple high-signal-intensity foci of varying size are seen within the mass and correspond to the hematopoietic component of a myelolipoma, which in this case forms a large part of the mass (cf **e**). **(e)** Photomicrograph (original magnification, ×100; H-E stain) (left) shows a myelolipoma with a capsule *(C)* superior to adrenocortical tissue *(A)*, the hyperfunctioning part of the lesion. More inferiorly, there is a mixture of vacuolated fat cells *(F)* and hematopoietic (bone marrow) cells *(H)*, which make up a large part of the myelolipoma. A higher-power photomicrograph of the same lesion (original magnification, ×200; H-E stain) (right) demonstrates a vacuolated fat cell *(F)* surrounded by markedly hyperchromatic hematopoietic cells.

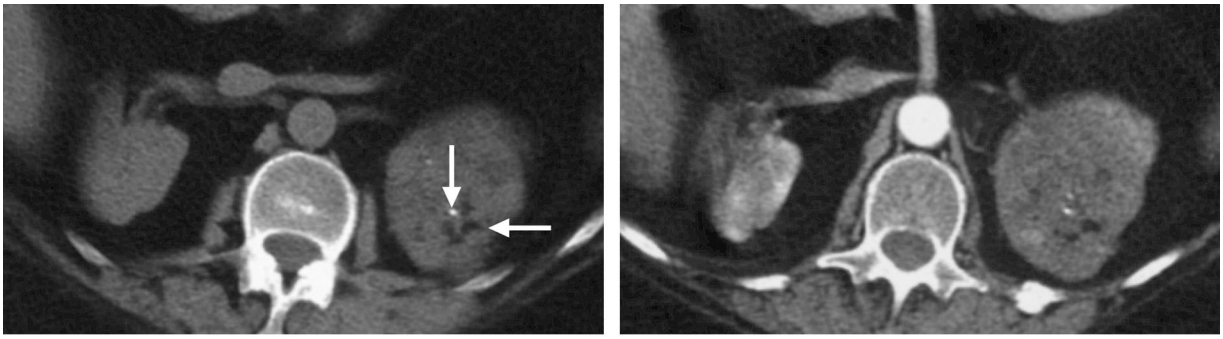

a. **b.**

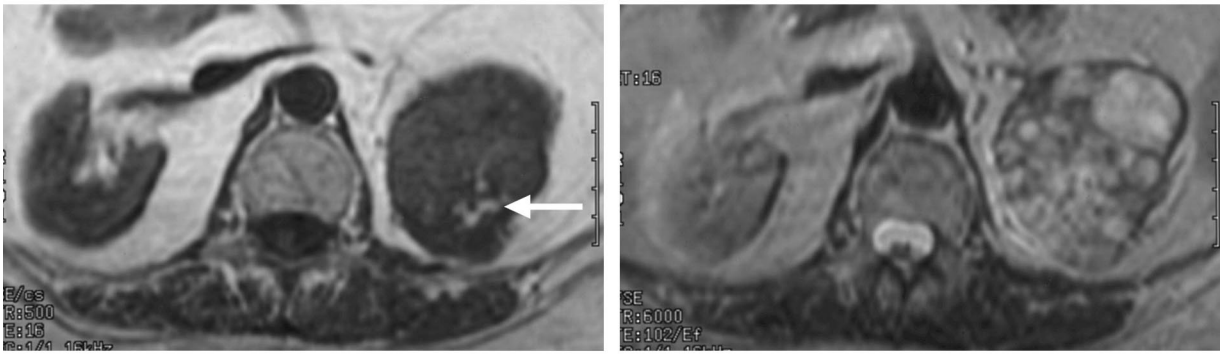

c. **d.**

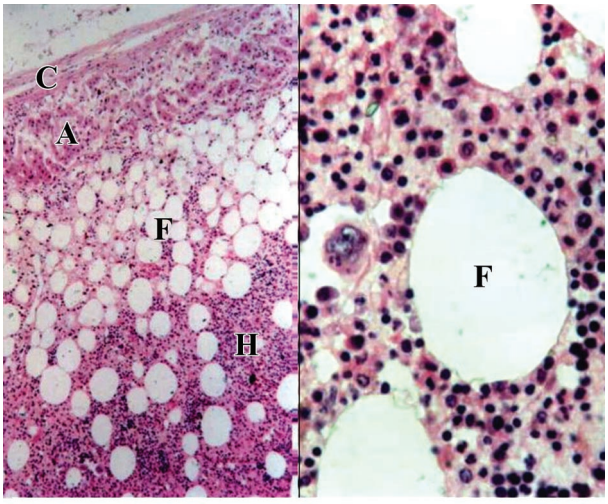

e.

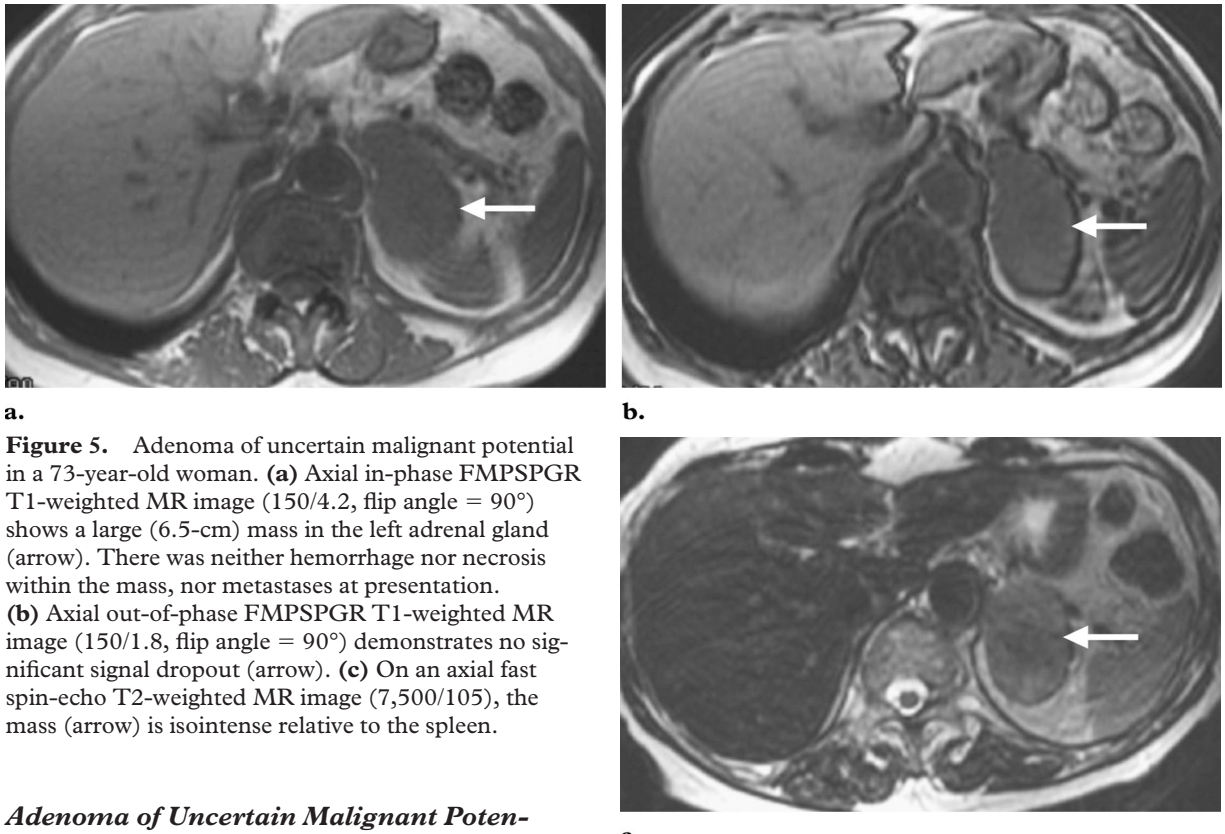

a. **b.** **c.**

Figure 5. Adenoma of uncertain malignant potential in a 73-year-old woman. **(a)** Axial in-phase FMPSPGR T1-weighted MR image (150/4.2, flip angle = 90°) shows a large (6.5-cm) mass in the left adrenal gland (arrow). There was neither hemorrhage nor necrosis within the mass, nor metastases at presentation. **(b)** Axial out-of-phase FMPSPGR T1-weighted MR image (150/1.8, flip angle = 90°) demonstrates no significant signal dropout (arrow). **(c)** On an axial fast spin-echo T2-weighted MR image (7,500/105), the mass (arrow) is isointense relative to the spleen.

Adenoma of Uncertain Malignant Potential.—In two of 37 cases, the adrenal lesion was classified histologically as an adenoma of uncertain malignant potential because some dysplastic features were identified (Fig 5). Both patients were over 70 years old, which is older than the mean age for patients with simple benign adenomas (45 years). The imaging features in these two cases were intermediate between benign and malignant features. The maximum diameters of the lesions (3.5 and 6.5 cm, respectively) were less than that of the smallest carcinoma. However, the unenhanced CT attenuation value was relatively high (38 HU) in the case in which CT findings were available, and there was minimal signal dropout at chemical shift imaging (4% and 9%, respectively). One patient subsequently developed metastases and died of the disease, indicating that the lesion was indeed malignant.

Carcinoma.—In 10 of 37 cases (27%), the adrenal lesion was a carcinoma. These carcinomas had a female predilection, and the mean patient age was similar to that of patients with adrenal adenomas (Tables 1, 2). All lesions had a maximum transverse diameter over 7.5 cm (mean, 14.5 cm; range, 7.5–21 cm), making them significantly larger than the adenomas ($P < .0001$) and adenomas of uncertain malignant potential ($P = .03$). The unenhanced CT attenuation values of the solid (nonnecrotic) parts of the tumor (mean, 28.1 HU; range, 20–31 HU) were significantly higher than those of the adenomas ($P = .048$). The tumors usually had a markedly heterogeneous texture at both CT and MR imaging (Figs 6–8). Necrosis was seen in nine of 10 cases

Figure 6. Adrenal carcinoma in a 32-year-old woman with Cushing syndrome. **(a)** Unenhanced CT scan demonstrates a large, low-attenuation suprarenal mass (short arrows) containing areas of high attenuation (long arrows) that are consistent with hemorrhage. **(b)** Contrast-enhanced CT scan demonstrates the mass with heterogeneous enhancement. Large areas of necrosis are also seen (*). Note the anterior displacement and compression of the inferior vena cava (IVC) (arrow). **(c)** Axial T1-weighted MR image (500/14) demonstrates high-signal-intensity areas within the mass (arrow), a finding that is consistent with hemorrhage. **(d)** Axial fast spin-echo T2-weighted MR image (7,500/100) also demonstrates extensive high-signal-intensity areas within the mass (arrow), a finding that is consistent with necrosis. **(e)** Photomicrograph (original magnification, ×100; H-E stain) demonstrates amorphous necrosis (arrows), a finding that is seen in the majority of adrenal carcinomas.

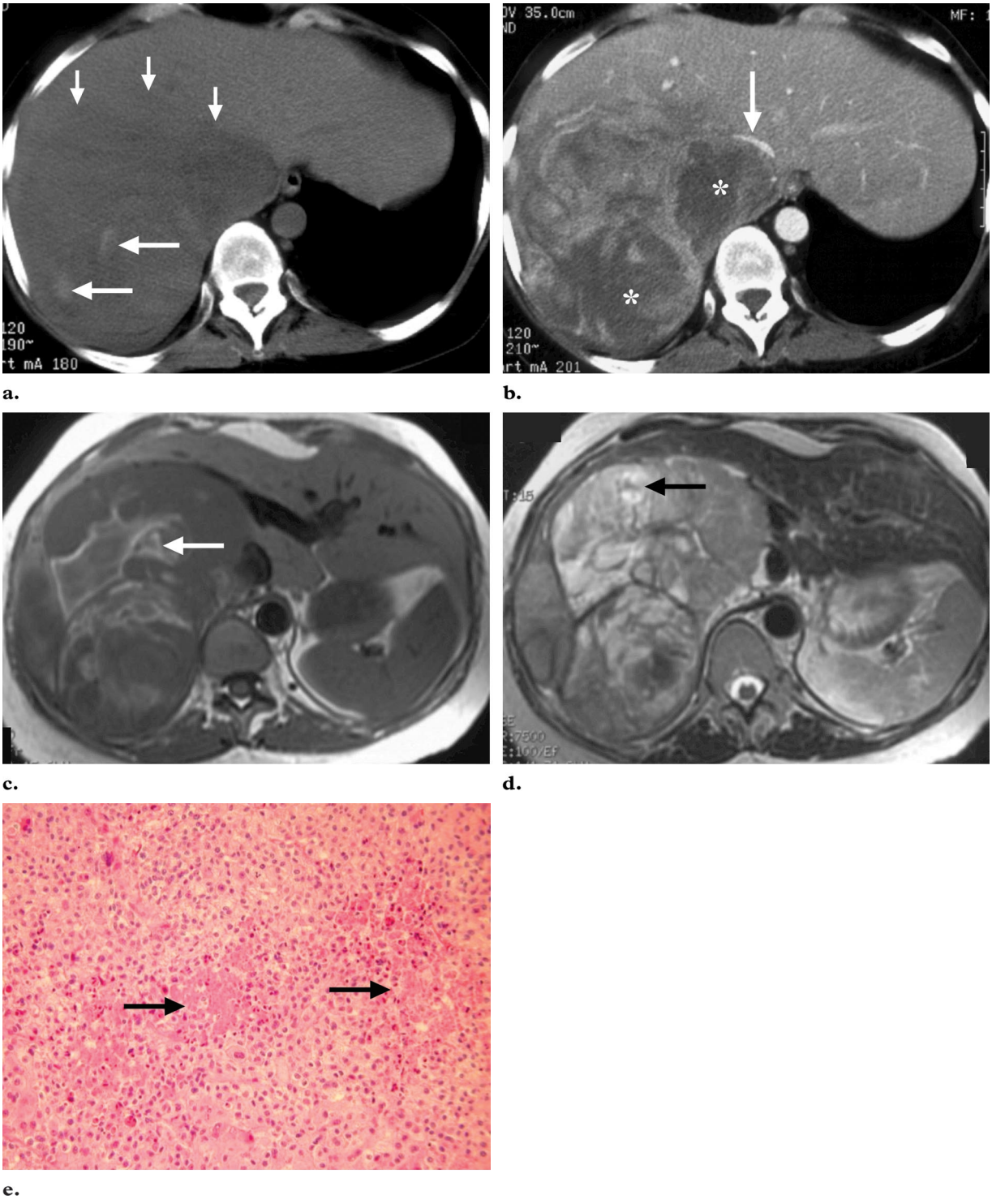

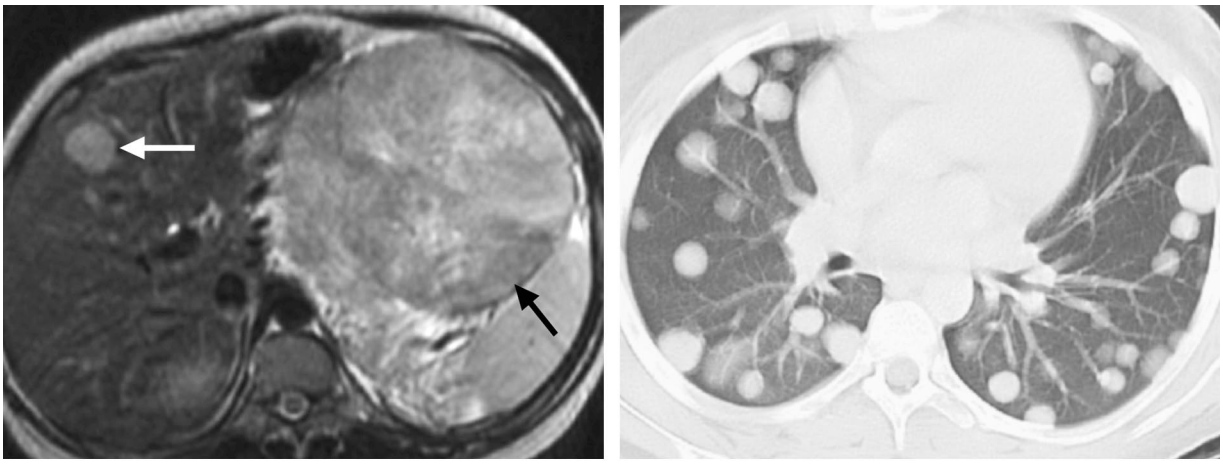

a. **b.**

Figure 7. Adrenal carcinoma in an 11-year-old girl with Cushing syndrome and virilization. **(a)** Axial fast spin-echo T2-weighted MR image (5,000/105) shows a large, left-sided adrenocortical carcinoma (black arrow) and a liver metastasis (white arrow). **(b)** Chest CT scan shows extensive lung metastases.

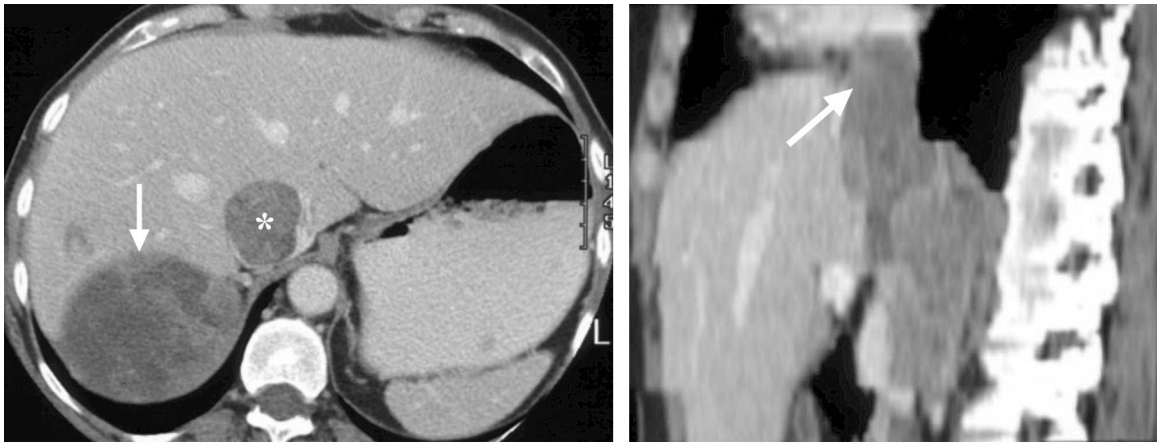

a. **b.**

Figure 8. Adrenocortical carcinoma in a 45-year-old woman with a history of hypertension. **(a)** Contrast-enhanced CT scan demonstrates a large, heterogeneously enhancing mass in the right suprarenal region (arrow) with extension into the IVC (*). **(b)** Sagittal thin-section reformatted image elegantly demonstrates tumor extension into the IVC and right atrium (arrow).

(Fig 6), and hemorrhage ($n = 4$) (Fig 6) or calcification ($n = 3$) was frequently identified. Contrast enhancement was mild and markedly heterogeneous (Figs 6, 8). At the time of presentation, six patients had lung or liver metastases (Fig 7) and four patients had tumor thrombus extending into the IVC and, in one case, invading the IVC wall (Fig 8).

Bilateral Adrenal Disease

The imaging features of these bilateral diseases are summarized in Tables 3 and 4.

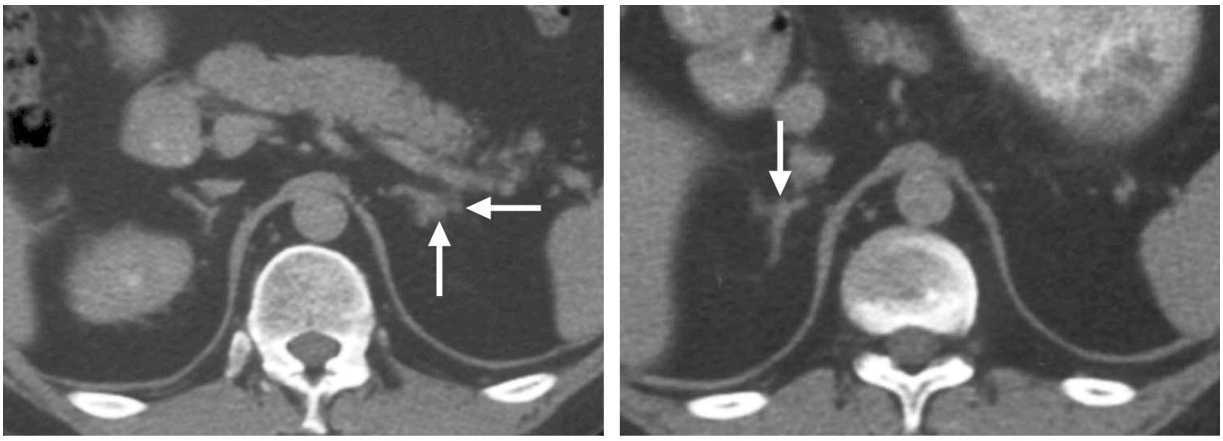

a. b.

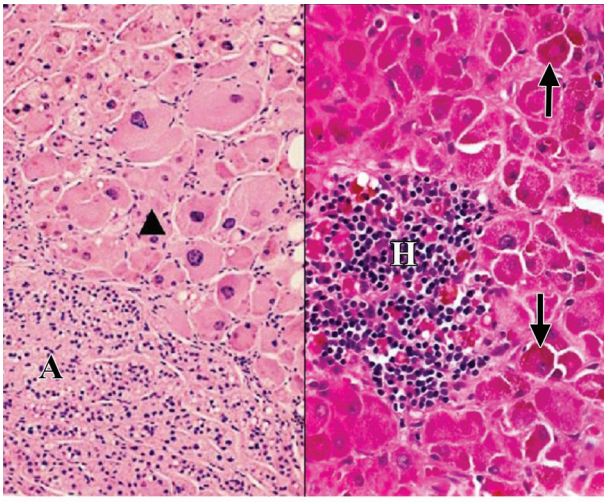

c.

Figure 9. PPNAD in a 28-year-old man. **(a, b)** Delayed contrast-enhanced CT scans show small nodules in the left **(a)** and right **(b)** adrenal glands (arrows). The remaining portions of the glands do not appear hyperplastic. **(c)** Photomicrograph (original magnification, ×200; H-E stain) (left) shows nodules of enlarged and hyperchromatic cells (hyperplastic adrenocortical cells) (arrowhead) alternating with normal adrenocortical parenchyma *(A)*. Photomicrograph (original magnification, ×200; H-E stain) (right) reveals deeply eosinophilic cells with an abundance of lipofuscin pigment (arrows) and a focal cluster of hyperchromatic cells with dark blue staining *(H)*. The latter are hematopoietic cells and are commonly seen incidentally in normal adrenal tissue. These findings indicate the presence of PPNAD, also known as micronodular hyperplasia.

PPNAD.—PPNAD was seen in two of 37 cases, both involving relatively young patients (10 and 28 years, respectively) (Fig 9). The adrenal glands manifested with bilateral small discrete nodules between 2 and 5 mm in size. The glands were not enlarged overall. In both cases, the diagnosis was confirmed histologically. In one case, the appearance was classical, with 2–5-mm pigmented nodules with atrophic intervening adrenal tissue (Fig 9). In the second case, the nodules were not pigmented but the features were otherwise characteristic. In this latter case, chemical shift imaging was available, and signal dropout was clearly visible.

AIMAH.—Imaging findings were available in only one case of AIMAH and were characteristic, with massively enlarged adrenal glands bilaterally, in this case retaining the normal adreniform shape. The adrenal limb width and maximum nodule size were 30 mm. Unlike with the adrenal adenomas and carcinomas, there was marked enhancement, predominantly of the periphery of the glands, at contrast-enhanced imaging (Fig 10a–10c). At MR imaging, the glands were isointense relative to the spleen and hypointense relative to the liver on T1-weighted images and hyperintense relative to both the spleen and the liver on T2-weighted images. The glands demonstrated 42% signal dropout at chemical shift imaging, suggesting the presence of intracellular lipid (Fig 10d, 10e). At histologic analysis, there were multiple large nodules interspersed with markedly hyperplastic adrenal tissue between the nodules. There was no pigmentation.

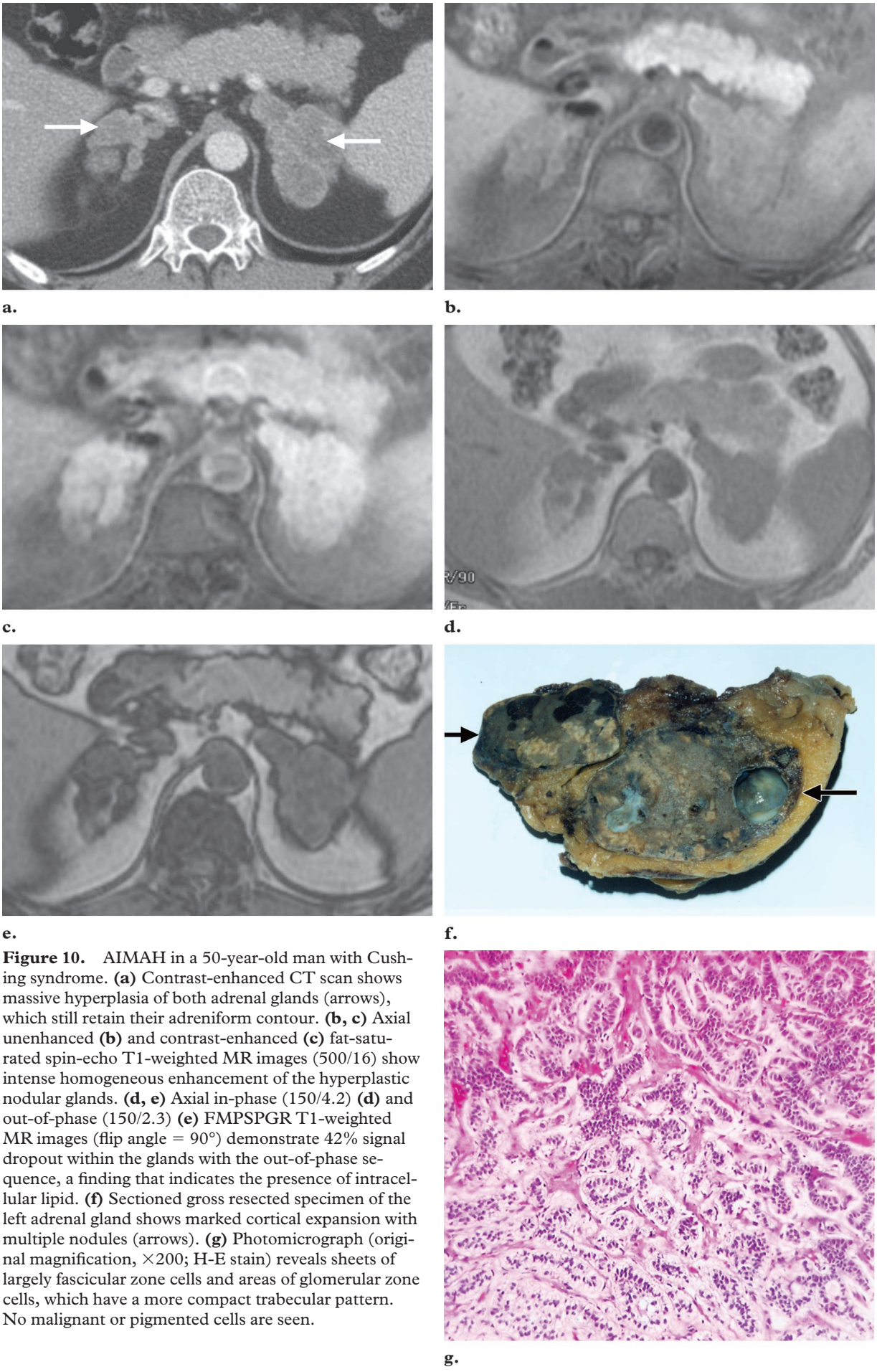

Figure 10. AIMAH in a 50-year-old man with Cushing syndrome. **(a)** Contrast-enhanced CT scan shows massive hyperplasia of both adrenal glands (arrows), which still retain their adreniform contour. **(b, c)** Axial unenhanced **(b)** and contrast-enhanced **(c)** fat-saturated spin-echo T1-weighted MR images (500/16) show intense homogeneous enhancement of the hyperplastic nodular glands. **(d, e)** Axial in-phase (150/4.2) **(d)** and out-of-phase (150/2.3) **(e)** FMPSPGR T1-weighted MR images (flip angle = 90°) demonstrate 42% signal dropout within the glands with the out-of-phase sequence, a finding that indicates the presence of intracellular lipid. **(f)** Sectioned gross resected specimen of the left adrenal gland shows marked cortical expansion with multiple nodules (arrows). **(g)** Photomicrograph (original magnification, ×200; H-E stain) reveals sheets of largely fascicular zone cells and areas of glomerular zone cells, which have a more compact trabecular pattern. No malignant or pigmented cells are seen.

Table 5
Comparison of Three Studies of Adrenocortical Carcinoma

	Didolkar et al, 1981 (16)	Soreide et al, 1992 (15)	Current Study
No. of cases	42	99	10
Median patient age (y)	53	54	43
Patient age range (y)	3–74	2–88	11–67
Proportion of clinically functioning tumors (%)	23.8	38.8	100
Female:male ratio in functioning tumors	9:1	2.25:1	2.33:1
Distant metastases at presentation (%)	52	50	60

Discussion

ACTH-independent Cushing syndrome is a rare disease that is always caused by a primary adrenal disease that secretes excessive cortisol. In our series, unilateral disease was most common, with adenomas (including adenomas within a myelolipoma and adenomas of uncertain malignant potential) and carcinomas accounting for 92% of cases, a finding that is consistent with those described in the literature (10).

Unilateral Disease

Hyperfunctioning adenomas, which accounted for the majority of cases in our series, had imaging features consistent with the reported CT and MR imaging appearances of other benign nonhyperfunctioning adrenal adenomas, being relatively small, homogeneous, and ovoid, with features consistent with intracellular lipid. Benign nonhyperfunctioning adenomas are usually less than 5 cm (mean, 2.4 cm) (8). The abundant intracellular lipid content of benign adenomas confers the low CT attenuation value and the typical signal dropout of 40% at chemical shift imaging (8,11). Thus, on the basis of imaging criteria alone, no distinction can be made between an adenoma causing primary adrenal Cushing syndrome and an incidentally discovered nonhyperfunctioning adenoma. Therefore, in patients with an incidentally discovered adenoma, clinical correlation (eg, biochemical or endocrinologic testing) is indicated to direct any further investigation. Lipid-poor hyperfunctioning adenoma is rare and was seen in only one of 20 cases (5%) in our series. Histologic analysis revealed a markedly pigmented gland (Fig 2).

An adrenal lesion with a macroscopic amount of fat is suggestive of a myelolipoma. Adrenal myelolipomas are rare benign tumors that are typically nonfunctioning and are composed of myeloid, erythroid, and fatty tissue, which may calcify. These lesions appear echogenic at ultrasonography and have fat attenuation at CT (Fig 3). At MR imaging, adrenal myelolipomas have high signal intensity on T1-weighted images and low signal intensity on fat-saturated images (Fig 3). When these features are seen, no further diagnostic tests are required. However, if there is a significant amount of associated soft tissue, a rare but recognized association of an adenoma with a myelolipoma should be considered. This entity has been described in association with Conn adenoma (12,13) but has also been described in Cushing syndrome caused by PPNAD (14). In both cases in our series in which the adenoma was within a myelolipoma, there was concern at the time of the initial report that there was an excess of soft tissue associated with the myelolipoma. Histologic analysis revealed that this soft tissue was the hypersecreting adenoma.

In two cases in our series, the adrenal lesion manifested histologically as an adenoma of uncertain malignant potential. This entity is not well described in the radiology literature. In our series, both lesions had some imaging features that were intermediate between those of an overt carcinoma and those of a benign adenoma. One lesion was relatively large for a benign lesion, with a relatively high attenuation value. In addition, there was virtually no signal dropout at chemical shift imaging in either lesion, indicating a lipid-poor composition. However, unlike with most of the malignancies, there was no evidence of necrosis, hemorrhage, or calcification and no evidence of metastatic disease at presentation. The diagnosis of a lesion of uncertain malignant potential could influence surgical management and is therefore of considerable preoperative importance.

Adrenocortical carcinoma is a rare, highly malignant tumor. The reported incidence in one series was 1.5 per 1 million persons per year (15), and in another series the tumor accounted for only 0.04% of all cancers registered at one institution over a 48-year period (16). The median age of affected patients is reported as 53 or 54 years (15,16), compared with a median age of 43 years in our series (Table 5). The adrenal carcinomas in our series demonstrated typical features, with a mean size of 14.5 cm, necrosis present in all but one lesion, and hemorrhage or calcification present in several lesions. The majority of affected

patients had evidence of metastatic disease at presentation, a finding that is similar to those in two large reported series (Table 5). This finding is interesting because one might expect hyperfunctioning carcinomas to manifest earlier than nonhyperfunctioning adrenal tumors. First, one would anticipate that patients with hyperfunctioning carcinoma would present earlier due to the clinical syndrome; and second, the hypersecreting tumors are more likely to be well differentiated (15,16). In our series, however, liver and lung metastases and tumor invasion of the IVC were seen in over one-half of patients.

Unilateral primary adrenal Cushing syndrome is treated surgically whenever possible. Confident preoperative distinction between benign and malignant adrenal lesions may improve surgical planning, allowing laparoscopic adrenalectomy, a minimally invasive surgical technique, to be undertaken safely. This approach, particularly in patients who may be obese secondary to Cushing syndrome, has lower postoperative morbidity and is the preferred treatment technique in nonmalignant lesions less than 6 cm in diameter (17). In lesions that are larger than 6 cm or that appear overtly malignant, an open approach is usually advised. However, in small lesions less than 6 cm but with features suggesting malignant potential, an oncologic surgical approach may be considered more appropriate. Thus, when some features of malignancy are demonstrated radiologically, it is worth bearing in mind the possibility of a histologic diagnosis of uncertain malignant potential while planning the surgical approach.

Bilateral Adrenal Lesions

Although rare, nodular hyperplasia of the adrenal gland has been described in association with ACTH-independent Cushing syndrome and may be due to AIMAH or PPNAD.

PPNAD.—PPNAD is a rare cause of Cushing syndrome that was first described by Chute et al in 1949 (18). PPNAD is also known as bilateral micronodular adenomatosis and micronodular adrenal disease (19,20) and is considered a benign condition, with ACTH-independent autonomous hypersecretion of cortisol.

The symptoms of cortisol excess are often mild, with a long interval between the onset of symptoms and diagnosis. PPNAD is also associated with Carney complex, which is characterized by cardiac myxomas, cutaneous myxomas, mammary fibroadenomas, spotty mucocutaneous pigmentation, primary pigmented nodular adrenocortical disease, testicular tumors, or a pituitary adenoma that secretes growth hormone (21). PPNAD is transmitted as an autosomal dominant trait. The cause of this disorder is unknown. There is some evidence from a study by Wulffraat et al (22) that PPNAD has an underlying autoimmune mechanism. An immunoglobulin that stimulates DNA synthesis from adrenocortical cells has been detected in the serum of patients with PPNAD. Other suggested possible underlying causes of PPNAD include adrenal cell migrational abnormalities, hamartoma formation, and a defect on chromosome 16.

PPNAD typically manifests in younger female patients with considerably less enlargement of the adrenal glands than is seen in AIMAH. Patients can present with hypertension and other typical cushingoid findings such as "buffalo hump," moon facies, lethargy, weight gain, and bruising following trivial trauma. There is no biochemical evidence of suppression of cortisol levels with a high-dose dexamethasone suppression test, with ACTH levels remaining undetectable.

Cross-sectional imaging may show normal to slightly hyperplastic adrenal glands with multiple small nodules, as in the two cases of PPNAD in our study. The nodules do not normally exceed 5 mm, but nodules up to 1–2 cm may be seen in older patients. In patients under 10 years old, the nodules are generally 0.5–3.0 mm in diameter and may not be detected with CT or MR imaging, but in older patients the nodules should be readily demonstrated with either technique. At MR imaging, the nodules have lower signal intensity than adjacent "atrophic" cortical tissue with both T1- and T2-weighted sequences (23). Bilateral increased uptake is seen at iodine-131 aldosterol scintigraphy in patients with PPNAD. The pituitary gland has a normal imaging appearance. It is worthwhile performing echocardiography to rule out cardiac myxomas in PPNAD patients with suspected Carney complex.

At histologic analysis, the adrenal glands may appear normal or slightly enlarged with multiple small, pigmented nodules. The adrenal glands maintain their adreniform shape, and their weight is also within normal limits. Abundant eosinophilic cytoplasm is seen in the adrenal cortical cells and shows diffuse distribution of a granular brown pigment called lipofuscin. The nodules are predominantly found in the fascicular and reticular zones (24). In most cases, the internodular cortex in patients with PPNAD demonstrates cortical atrophy.

Bilateral adrenalectomy is the recommended and curative treatment for PPNAD (25). Initial management of PPNAD may be medical, with the aim being to suppress high levels of circulating cortisol with agents such as metyrapone or ketaconazole. However, the definitive treatment is adrenalectomy, followed by replacement with corticosteroids for life. Family screening is also recommended.

AIMAH.—AIMAH, first described by Kirschner et al (26) in 1964, is a rare disease with unique clinical, endocrinologic, and histopathologic features. Clinical manifestations, which are described in varying degrees of detail in the case reports, include hypertension, weight gain, impaired glucose tolerance or diabetes mellitus, osteoporosis, and easy bruisability. Hypogonadism and gynecomastia have been reported in males and hirsutism in females. There have also been case reports of proximal myopathy, psychiatric disturbances, and infection (27). The clinical characteristics of this condition include a male predilection and a higher mean patient age compared with adenomas, with typical biochemical abnormalities of ACTH-independent Cushing syndrome.

The pathogenesis of AIMAH is unclear, and a number of theories have been proposed to explain the development of massive adrenal enlargement. An early hypothesis held that chronic stimulation of the adrenal cortex in long-standing Cushing disease ultimately resulted in autonomous adrenal cortisol production (28). Other investigators have proposed a transition from ACTH dependence to ACTH independence as a pathogenic mechanism, although the lack of development of Nelson syndrome (enlarging pituitary tumor, increased skin pigmentation, and rising levels of ACTH seen after bilateral adrenalectomy for Cushing disease) after bilateral adrenalectomy in patients with AIMAH argues against this being the underlying cause. The possibility that stimulators of the adrenal cortex other than ACTH may play a role in the pathogenesis of AIMAH is also suggested by the results of dynamic testing in several case reports. In this context, gastric inhibitory polypeptide (GIP)–induced Cushing syndrome has been reported. GIP-mediated food-dependent Cushing syndrome is believed to result from the ectopic expression of GIP receptors by adrenocortical cells (29). A similar mechanism has also been reported with vasopressin and β-adrenergic receptors.

The adrenal glands in patients with AIMAH have a dramatic CT appearance. Both glands are massively enlarged, with multiple macronodules measuring up to 5 cm in diameter. MR imaging features have also been well described. The large nodules are isointense relative to muscle with T1-weighted sequences and hyperintense relative to liver with T2-weighted sequences. In contrast, the nodules in pituitary-dependent macronodular hyperplasia have a signal intensity similar to that of liver on T2-weighted MR images (30). The case of AIMAH in our series supports this finding. In addition, our case demonstrated marked signal dropout at out-of-phase chemical shift MR imaging, a finding that is consistent with a lipid-rich composition. At CT and MR imaging of the brain, the pituitary gland has a normal appearance. I-131–labeled adrenal scintigraphy shows bilateral increased uptake.

Histologic examination demonstrates a remarkable increase in the number of small clear cells, which are mostly derived from the upper fascicular zone. The amount of cortisol produced by each cell is slight, so that significant enlargement of the adrenal gland is necessary before excessive cortisol production causes Cushing syndrome (31). There is no evidence of malignancy or invasion. The status of the internodular uninvolved adrenal cortex is controversial. The tissue is difficult to identify due to the grossly distorted glands. Normal, atrophic, or uninvolved and hyperplastic cortex has been reported by different investigators. In patients with ACTH-dependent macronodular hyperplasia associated with Cushing disease or with ectopic ACTH production, the internodular cortex is always hyperplastic (32). Each adrenal gland in patients with AIMAH weighs about 96 g ± 16.7, compared with a normal weight of 4–6 g (33).

The current treatment of choice is bilateral complete adrenalectomy. Recent reports have also suggested laparoscopic adrenalectomy for affected patients (34).

Conclusions

Imaging plays an important role in identifying the underlying disease when a biochemical diagnosis of ACTH-independent Cushing syndrome is made. Knowledge of the range of imaging appearances of the adrenal glands in primary adrenal Cushing syndrome may allow definitive diagnosis in the majority of cases. The initial distinction between unilateral and bilateral disease is usually straightforward. In unilateral disease, a confident diagnosis of benign or malignant disease can be made in most cases. This distinction is helpful in optimizing surgical planning. In bilateral disease, the marked differences in imaging characteristics between PPNAD and AIMAH allow the radiologist to confidently diagnose these rare diseases.

References

1. Nieman LK, Cutler GB Jr. Cushing's syndrome. In: DeGroot LJ, ed. Endocrinology. Philadelphia, Pa: Saunders, 1995; 1741–1770.
2. Sohaib SA, Hanson JA, Newell-Price JD, et al. CT appearance of the adrenal glands in adrenocorticotrophic hormone-dependent Cushing's syndrome. AJR Am J Roentgenol 1999; 172:997–1002.
3. Doppman JL, Chrousos GP, Papanicolaou DA, Stratakis CA, Alexander HR, Nieman LK. Adrenocorticotropin-independent macronodular adrenal hyperplasia: an uncommon cause of primary adrenal hypercortisolism. Radiology 2000; 216: 797–802.

4. Doppman JL, Travis WD, Nieman L, et al. Cushing syndrome due to primary pigmented nodular adrenocortical disease: findings at CT and MR imaging. Radiology 1989; 172:415–420.
5. Newell-Price J, Trainer P, Besser M, Grossman A. The diagnosis and differential diagnosis of Cushing's syndrome and pseudo-Cushing's states. Endocr Rev 1998; 19:647–672.
6. Aubert S, Wacrenier A, Leroy X, et al. Weiss system revisited: a clinicopathologic and immunohistochemical study of 49 adrenocortical tumors. Am J Surg Pathol 2002; 26:1612–1619.
7. Lloyd RV, Douglas BR, Young WR. Endocrine diseases. Washington, DC: American Registry of Pathology and the Armed Forces Institute of Pathology, 2002.
8. Korobkin M, Brodeur FJ, Yutzy GG, et al. Differentiation of adrenal adenomas from nonadenomas using CT attenuation values. AJR Am J Roentgenol 1996; 166:531–536.
9. Allan CA, Kaltsas G, Perry L, et al. Concurrent secretion of aldosterone and cortisol from an adrenal adenoma-value of MRI in diagnosis. Clin Endocrinol (Oxf) 2000; 53:749–753.
10. Blevins LS. Cushing's syndrome due to adrenal disorders. In: Blevins LS, ed. Cushing's syndrome. Norwell, Mass: Kluwer Academic Publishers, 2003; 201–228.
11. Korobkin M, Giordano TJ, Brodeur FJ, et al. Adrenal adenomas: relationship between histologic lipid and CT and MR findings. Radiology 1996; 200:743–747.
12. Cormio L, Ruutu M, Giardina C, Selvaggi FP. Combined adrenal adenoma and myelolipoma in a patient with Conn syndrome: case report. Panminerva Med 1992; 34:209–212.
13. Lazurova I, Sokol L, Trejbal D, Bober J, Zachar M, Pajtasova D. Aldosterone-producing adenoma associated with foci of myelolipoma. Wien Klin Wochenschr 1998; 110:379–381.
14. Reza-Albarran AA, Gomez-Perez FJ, Lopez JC, et al. Myelolipoma: a new adrenal finding in Carney's complex? Endocr Pathol 1999; 10:251–257.
15. Soreide JA, Brabrand K, Thoresen SO. Adrenal cortical carcinoma in Norway, 1970–1984. World J Surg 1992; 16:663–667.
16. Didolkar MS, Bescher RA, Elias EG, Moore RH. Natural history of adrenal cortical carcinoma: a clinicopathologic study of 42 patients. Cancer 1981; 47:2153–2161.
17. Prager G, Heinz-Peer G, Passler C, et al. Surgical strategy in adrenal masses. Eur J Radiol 2002; 41: 70–77.
18. Chute AL, Robinson GC, Donohue WL. Cushing's syndrome in children. J Pediatr 1949; 34:20–39.
19. Kracht J, Tamm J. Bilaterale kleinknotige Adenomatose der Nebennierenrinde bei Cushing Syndrom. Virchows Arch Pathol Anat 1960; 333:1–9.
20. Ruder HJ, Loriaux DL, Lipsett MB. Severe osteopenia in young adults associated with Cushing's syndrome due to micronodular adrenal disease. J Clin Endocrinol Metab 1974; 39:1138–1147.
21. Bain J. "Carney's complex" (letter). Mayo Clin Proc 1986; 61:508.
22. Wulffraat NM, Drexhage HA, Wiersinga WM, van der Gaag RD, Jeucken P, Mol JA. Immunoglobulins of patients with Cushing's syndrome due to pigmented adrenocortical micronodular dysplasia stimulate in vitro steroidogenesis. J Clin Endocrinol Metab 1988; 66:301–307.
23. Peppercorn PD, Reznek RH. State-of-the-art CT and MRI of the adrenal gland. Eur Radiol 1997; 7:822–836.
24. Kohler G, Anding K, Bohm N. Primary pigmented nodular adrenocortical dysplasia. Pathol Res Pract 1998; 194:201–204.
25. Carney JA. Carney complex: the complex of myxomas, spotty pigmentation, endocrine overactivity, and schwannomas. Semin Dermatol 1995; 14:90–98.
26. Kirschner MA, Powell RDJ, Lipsett MB. Cushing's syndrome: nodular cortical hyperplasia of adrenal glands with clinical and pathological features suggesting adrenocortical tumours. J Clin Endocrinol Metab 1964; 24:947.
27. Lieberman SA, Eccleshall TR, Feldman D. ACTH-independent massive bilateral adrenal disease (AIMBAD): a subtype of Cushing's syndrome with major diagnostic and therapeutic implications. Eur J Endocrinol 1994; 131:67–73.
28. Smals AG, Pieters GF, van Haelst UJ, Kloppenborg PW. Macronodular adrenocortical hyperplasia in long-standing Cushing's disease. J Clin Endocrinol Metab 1984; 58:25–31.
29. Reznik Y, Allali-Zerah V, Chayvialle JA, et al. Food-dependent Cushing's syndrome mediated by aberrant adrenal sensitivity to gastric inhibitory polypeptide. N Engl J Med 1992; 327:981–986.
30. Doppman JL, Nieman LK, Travis WD, et al. CT and MR imaging of massive macronodular adrenocortical disease: a rare cause of autonomous primary adrenal hypercortisolism. J Comput Assist Tomogr 1991; 15:773–779.
31. Aiba M. Cushing's syndrome due to huge bilateral adrenocortical multinodular hyperplasia: ACTH-independent bilateral adrenocortical macronodular hyperplasia (AIMAH). Nippon Naibunpi Gakkai Zasshi 1994; 70:37–42.
32. Doppman JL, Miller DL, Dwyer AJ, et al. Macronodular adrenal hyperplasia in Cushing disease. Radiology 1988; 166:347–352.
33. Neville AM, O'Hare MJ. Histopathology of the human adrenal cortex. Clin Endocrinol Metab 1985; 14:791–820.
34. Shinojima H, Kakizaki H, Usuki T, Harabayashi T, Ameda K, Koyanagi T. Clinical and endocrinological features of adrenocorticotropic hormone-independent bilateral macronodular adrenocortical hyperplasia. J Urol 2001; 166:1639–1642.

This article meets the criteria for 1.0 credit hour in category 1 of the AMA Physician's Recognition Award. To obtain credit, see accompanying test at http://www.rsna.org/education/rg_cme.html.